European Conference on Computational Fluid Dynamics
ECCOMAS CFD 2006
P. Wesseling, E. Oñate and J. Périaux (Eds)

CONTROLLABILITY TECHNIQUES FOR THE HELMHOLTZ EQUATION WITH SPECTRAL ELEMENTS

Erkki Heikkola[1], Sanna Mönkölä[2,*], Anssi Pennanen[2], Tuomo Rossi[2]

[1]Numerola Oy, P.O. Box 126, FI-40101 Jyväskylä, Finland
e-mail: erkki.heikkola@numerola.fi

[2]Department of Mathematical Information Technology
University of Jyväskylä, P.O. Box 35 (Agora)
FI-40014 University of Jyväskylä, Jyväskylä, Finland
*e-mail: sanna.monkola@it.jyu.fi

Key words: Exact controllability, Helmholtz equation, Spectral element method.

Abstract. *We consider the use of controllability techniques to solve the Helmholtz equation. Instead of solving directly the time-harmonic equation, we formulate the Helmholtz problem as an exact controllability problem for the time-dependent wave equation. This involves finding such initial conditions that after one time-period the solution and its time derivative would coincide with the initial conditions. The problem is formulated as a least-squares optimization problem, which is solved by a preconditioned conjugate gradient method. We use spectral elements for spatial discretization and the classical fourth order Runge-Kutta method for time discretization. This leads to high accuracy and diagonal mass matrices. Mass lumping makes the explicit time-stepping scheme for the wave equation very efficient.*

1 INTRODUCTION

We consider controllability methods for the numerical solution of the two-dimensional Helmholtz equation with an absorbing boundary condition describing the scattering of a time-harmonic incident wave by a sound-soft obstacle:

$$-\omega^2 U - \nabla^2 U = 0, \qquad \text{in } \Omega, \tag{1}$$

$$U = 0, \qquad \text{on } \Gamma_0, \tag{2}$$

$$-i\omega U + \frac{\partial U}{\partial \mathbf{n}} = G_{\text{ext}}, \qquad \text{on } \Gamma_{\text{ext}}, \tag{3}$$

where $U(\mathbf{x})$ denotes the total acoustic pressure consisting of the scattered wave $U_{\text{scat}}(\mathbf{x})$ and the incident wave $U_{\text{inc}}(\mathbf{x}) = \exp(i\vec{\omega}\cdot\mathbf{x})$, where i is the imaginary unit and the vector $\vec{\omega}$ gives the propagation direction. The function G_{ext} depends on the incident wave. The

domain Ω is bounded by the surface of the obstacle Γ_0 and an absorbing boundary Γ_{ext}. Vector $\mathbf{n}$ is the outward normal vector to domain Ω. In this case, the angular frequency $\omega = \|\vec{\omega}\|_2$ is equal to the wavenumber, and it is related to the wavelength λ by the formula $\lambda = \frac{2\pi}{\omega}$.

Spatial discretization is done with spectral element method (SEM). It allows convenient treatment of complex geometries. The basis functions are higher order Lagrange interpolation polynomials, and the nodes of these functions are placed at Gauss-Lobatto collocation points. The integrals in the weak form of the equation are evaluated with the corresponding Gauss-Lobatto quadrature formulas. As a consequence of the choice, spectral element discretization leads to diagonal mass matrices also with a higher-order basis[1]. This significantly improves the computational efficiency of the explicit time-integration used. Moreover, when using higher order elements, same accuracy is reached with less degrees of freedom than when using lower order finite elements[2].

After discretization, the controllability problem is reformulated as a least-squares optimization problem, which is solved with a preconditioned conjugate gradient algorithm. Such an approach was first suggested and developed in the 1990s by French researchers[3] and we have recently introduced some improvements to its practical realization[4]. In these references, the central finite difference scheme, which is only second-order accurate with respect to time step, has been used for time discretization. When higher order elements are used with the second order time discretization, the error of time discretization dominates reducing the global accuracy of the scheme, unless very small time steps are considered. In this article, we improve the accuracy of the method by using the fourth order accurate Runge-Kutta method for time discretization. We also compare it with the method with central finite difference scheme[4].

2 EXACT CONTROLLABILITY FORMULATION

In order to solve the Helmholtz problem (1)-(3), we return to the time-dependent wave equation. Direct time-integration of the wave equation could be used to reach the time-periodic case, but convergence is usually too slow to be useful in practice. This is why we use an alternative idea of Bristeau, Glowinski and Périaux to speed up the convergence by control techniques[3].

The original time-harmonic equation is reformulated as an exact controllability[5] problem for the wave equation: Find initial conditions e_0 and e_1 such that:

$$\frac{\partial^2 u}{\partial t^2} - \nabla^2 u = 0, \qquad \text{in } Q = \Omega \times [0,T], \tag{4}$$

$$u = 0, \qquad \text{on } \gamma_0 = \Gamma_0 \times [0,T], \tag{5}$$

$$\frac{\partial u}{\partial t} + \frac{\partial u}{\partial \mathbf{n}} = g_{\text{ext}}, \qquad \text{on } \gamma_{\text{ext}} = \Gamma_{\text{ext}} \times [0,T], \tag{6}$$

$$u(\mathbf{x},0) = e_0, \quad \frac{\partial u}{\partial t}(\mathbf{x},0) = e_1, \qquad \text{in } \Omega, \tag{7}$$

$$u(\mathbf{x},T) = e_0, \quad \frac{\partial u}{\partial t}(\mathbf{x},T) = e_1, \qquad \text{in } \Omega. \tag{8}$$

The key idea of the method is to look for a time periodic solution by using initial conditions as control variables. Once the exact controllability problem is solved, the real-valued initial conditions are equal to the terminal conditions, and T-periodic solution u is found. The complex-valued solution U of (1)-(3) is then obtained by $U = e_0 + \frac{i}{\omega} e_1$.

3 SPECTRAL ELEMENT DISCRETIZATION

For the spatial discretization of the wave equation (4)-(7), we use the spectral element method, which combines the geometric flexibility of classical finite elements with the high accuracy of spectral methods. The spectral element discretization of the problem is based on the weak formulation of the classical wave equation (4)-(6): Find u satisfying $u(t) \in V = \{v \in H^1(\Omega) \text{ such that } v = 0 \text{ on } \Gamma_0\}$ for any $t \in [0,T]$ and

$$\int_\Omega \frac{\partial^2 u}{\partial t^2} v \, dx + \int_\Omega \nabla u \cdot \nabla v \, dx + \int_{\Gamma_{\text{ext}}} \frac{\partial u}{\partial t} v \, ds = \int_{\Gamma_{\text{ext}}} g_{\text{ext}} v \, ds \tag{9}$$

for any $v \in V$ and $t \in [0,T]$.

The computational domain Ω is divided into N_e quadrilateral elements Ω_i, $i = 1, \ldots, N_e$ such that $\Omega = \bigcup_{i=1}^{N_e} \Omega_i$. For the discrete formulation, we define the reference element $\Omega_{\text{ref}} = [0,1]^2$ and affine mappings $\mathcal{G}_i : \Omega_{\text{ref}} \to \Omega_i$ such that $\mathcal{G}_i(\Omega_{\text{ref}}) = \Omega_i$. Then, the finite element subspace $\mathbf{V}_h^r$ of $\mathbf{V}$ is given by $V_h^r = \{v_h \in V \text{ such that } v_h|_{\Omega_i} \circ \mathcal{G}_i \in Q^r\}$, where $Q^r(\Omega_i) = \{v(\xi,\zeta) = \sum_{p=0}^r \sum_{q=0}^r a_{pq} \xi^p \zeta^q, \ a_{pq} \in \mathbb{R}\}$ is the set of polynomials of order r in $\mathbb{R}^2$.

After spatial discretization we have the semi-discrete equation

$$\mathcal{M} \frac{\partial^2 \mathbf{u}}{\partial t^2} + \mathcal{S} \frac{\partial \mathbf{u}}{\partial t} + \mathcal{K}\mathbf{u} = \mathcal{F}, \tag{10}$$

where vector $\mathbf{u}(t)$ contains the nodal values of the function $u(\mathbf{x},t)$ at time t, and satisfies the initial condition (7) at time $t = 0$. Because matrices $\mathcal{M}$ and $\mathcal{S}$ are diagonal, explicit time stepping requires only matrix-vector multiplications. Stiffness matrix is denoted by $\mathcal{K}$, and $\mathcal{F}$ is the vector due to the function g_{ext}.

4 TIME DISCRETIZATION

We use the fourth order Runge-Kutta scheme for time discretization. This scheme is fourth order accurate and with a diagonal mass matrix also fully explicit, which are both essential properties for computational efficiency. Only matrix-vector products are needed in time-dependent simulation, but the scheme needs to satisfy the stability condition,

which limits the length of the time step. We have chosen to divide the time interval $[0, T]$ into N time steps, each of size $\Delta t = T/N$.

After applying the fourth order Runge-Kutta scheme to equation (10) and taking into account the initial conditions (7) we obtain the fully discrete state equation, which can be represented in the matrix form

$$\begin{pmatrix} \mathcal{I} & & & & \\ \mathcal{N} & \mathcal{I} & & & \\ & \ddots & \ddots & & \\ & & \mathcal{N} & \mathcal{I} & \\ & & & \mathcal{N} & \mathcal{I} \end{pmatrix} \begin{pmatrix} y^0 \\ y^1 \\ \vdots \\ y^{N-1} \\ y^N \end{pmatrix} - \begin{pmatrix} \mathcal{I} \\ 0 \\ \vdots \\ 0 \\ 0 \end{pmatrix} \begin{pmatrix} e_0 \\ e_1 \end{pmatrix} - \begin{pmatrix} 0 \\ \hat{F}^1 \\ \vdots \\ \hat{F}^{N-1} \\ \hat{F}^N \end{pmatrix} = 0, \qquad (11)$$

where $y^0 = (e_0, e_1)^T$. The vector block $y^i = \left(u^i, \frac{\partial u^i}{\partial t}\right)^T$, $i = 1, \ldots, N$, contains the vector u and its first time derivative at time $i\Delta t$. The identity matrix is denoted by $\mathcal{I}$, and the other matrix and vector blocks in (11) are given by $\mathcal{N} = -(\hat{B}\hat{A}^{-1}\hat{C} + \mathcal{I})$ and $\hat{F}^i = -\hat{B}\hat{A}^{-1}\hat{H}$ such that $\hat{B} = \begin{pmatrix} \hat{R} & 2\hat{R} & 2\hat{R} & \hat{R} \end{pmatrix}$ and $\hat{H}^T = \Delta t \mathcal{M}^{-1} \begin{pmatrix} \mathcal{F}^{i-1} & 0 & \mathcal{F}^{i-\frac{1}{2}} & 0 & \mathcal{F}^{i-\frac{1}{2}} & 0 & \mathcal{F}^{i} & 0 \end{pmatrix}$, where $\mathcal{F}^i$ is the vector $\mathcal{F}$ at time $i\Delta t$. To compute the matrix and vector blocks mentioned above, also the following block forms are defined:

$$\hat{A} = \begin{pmatrix} \mathcal{I} & & & \\ \hat{D} & \mathcal{I} & & \\ & \hat{D} & \mathcal{I} & \\ & & 2\hat{D} & \mathcal{I} \end{pmatrix}, \qquad \hat{C} = \begin{pmatrix} 2\hat{D} \\ 2\hat{D} \\ 2\hat{D} \\ 2\hat{D} \end{pmatrix},$$

$$\hat{D} = \begin{pmatrix} 0 & -\frac{\Delta t}{2}\mathcal{I} \\ \frac{\Delta t}{2}\mathcal{M}^{-1}\mathcal{K} & \frac{\Delta t}{2}\mathcal{M}^{-1}\mathcal{S} \end{pmatrix}, \qquad \hat{R} = \begin{pmatrix} -\frac{1}{6}\mathcal{I} & 0 \\ 0 & -\frac{1}{6}\mathcal{I} \end{pmatrix}.$$

5 LEAST SQUARES PROBLEM

The exact controllability problem for computing $T-$periodic solution for the wave equation involves finding such initial conditions e_0 and e_1 that the solution u and its time derivative $\frac{\partial u}{\partial t}$ at time T would coincide with the initial conditions. For the numerical solution, the exact controllability problem is replaced by a least-squares optimization problem with the functional J, which is, on the semi-discrete level, of the form:

$$J(e_0, e_1, \mathbf{u}) = \frac{1}{2}\left((\mathbf{u}(t) - e_0)^T \mathcal{K} (\mathbf{u}(t) - e_0) + \left(\frac{\partial \mathbf{u}(t)}{\partial t} - e_1\right)^T \mathcal{M} \left(\frac{\partial \mathbf{u}(t)}{\partial t} - e_1\right)\right). \qquad (12)$$

The purpose is to minimize functional J, which depends on the initial conditions both directly and indirectly through the solution of the wave equation.

5.1 Gradient of the cost function

Since vector $\mathbf{u}$ depends linearly on the initial conditions e_0 and e_1, J is a quadratic function, and (12) can be minimized by solving the linear system $\nabla J(e_0, e_1) = 0$ with a conjugate gradient (CG) method. For this, we compute the gradient of the discretized cost function (12) by the adjoint equation technique.

The adjoint equation corresponding to the state equation (11) is

$$\begin{pmatrix} \mathcal{I} & \mathcal{N}^T & & & \\ & \mathcal{I} & \mathcal{N}^T & & \\ & \ddots & \ddots & & \\ & & & \mathcal{I} & \mathcal{N}^T \\ & & & & \mathcal{I} \end{pmatrix} \begin{pmatrix} q^0 \\ q^1 \\ \vdots \\ q^{N-1} \\ q^N \end{pmatrix} = \begin{pmatrix} 0 \\ 0 \\ \vdots \\ 0 \\ \frac{\partial J(e_0, e_1, \mathbf{u}(e_0, e_1))}{\partial y^N} \end{pmatrix}, \tag{13}$$

where $q^i = \left(p^i, \frac{\partial p^i}{\partial t}\right)$, $i = N-1, \ldots, 0$, $\mathcal{N}^T = -(\hat{C}^T(\hat{A}^T)^{-1}\hat{B} + \mathcal{I})$, and

$$\frac{\partial J(e_0, e_1, \mathbf{u}(e_0, e_1))}{\partial y^N} = \begin{pmatrix} \frac{\partial J(e_0, e_1, \mathbf{u}(e_0, e_1))}{\partial u^N} \\ \frac{\partial J(e_0, e_1, \mathbf{u}(e_0, e_1))}{\partial \left(\frac{\partial u^N}{\partial t}\right)} \end{pmatrix} = \begin{pmatrix} \mathcal{K}(u^N - e_0) \\ \mathcal{M}(\frac{\partial u^N}{\partial t} - e_1) \end{pmatrix}. \tag{14}$$

Then, the gradient components are

$$\frac{dJ(e_0, e_1, \mathbf{u}(e_0, e_1))}{de_0} = \mathcal{K}(e_0 - u^N) + p^0, \tag{15}$$

$$\frac{dJ(e_0, e_1, \mathbf{u}(e_0, e_1))}{de_1} = \mathcal{M}\left(e_1 - \frac{\partial u^N}{\partial t}\right) + \frac{\partial p^0}{\partial t}. \tag{16}$$

5.2 Preconditioned conjugate gradient method

If the unpreconditioned CG algorithm is used, the number of iterations grows with the order of elements[6]. That is why we solve the least-squares problem with a preconditioned CG algorithm. The initial approximations of e_0 and e_1 are computed by using a transition procedure[7]. Each CG iteration step requires computation of the gradient ∇J, which involves the solution of the wave equation (4)-(8) and its adjoint equation. Also solution of one linear system with a preconditioner $\mathcal{L}$ and some matrix-vector operations are needed at each iteration.

We use the block-diagonal preconditioner

$$\mathcal{L} = \begin{pmatrix} \mathcal{K} & 0 \\ 0 & \mathcal{M} \end{pmatrix}, \tag{17}$$

where the first and second blocks are associated with the first and second terms in (12), respectively. Solution of a linear system with the block-diagonal preconditioner incorporates the solution of systems with the stiffness matrix $\mathcal{K}$ and the diagonal mass matrix $\mathcal{M}$. Efficient method for computing solution of linear systems with the matrix $\mathcal{K}$ is critical for the overall efficiency of the control method. We apply a modification of Kickinger's[8] algebraic multigrid (AMG). In this method coarsening (i.e. selection of the unknowns for coarser levels) is based on the graph of the stiffness matrix, instead of using actual values stored in the stiffness matrix[9]. The coarsening process operates in a geometric fashion by sequentially choosing a coarse node and eliminating the neighboring nodes of the graph. The primary criterion used here for selecting the next coarse grid node is to take the node with minimum degree (taking into account the eliminations). The secondary criterion is to follow the original numbering. This approach ensures fast computation of coarser level components. It also is an easy task to extend this method to use any graph related to the problem.

However, this strategy leads to far too coarse systems when applied to the graph of stiffness matrix obtained by higher-order discretization. This is due to increasing amount of connections between unknowns of the problem. Consequently, convergence factor of AMG degrades rapidly as the order of the approximation polynomials increases. We have overcome this problem by employing a graph that is constructed so that unknowns are connected to each other as lower-order element would have been used in the discretization process, i.e. only the unknowns corresponding to the nearest neighbouring nodes are connected to each other. The use of AMG methods for problems discretized with spectral elements has recently been studied in an article by Heys, Manteuffel, McCormick, and Olson[10], in which they applied the well-known AMG of Ruge and Stüben[11] to Poisson problem and Stokes equations.

6 NUMERICAL EXAMPLES

We consider a two-dimensional scattering problem (4)-(8) with $g_{\text{ext}} = \frac{\partial u_{\text{inc}}}{\partial \mathbf{n}} + \frac{\partial u_{\text{inc}}}{\partial t}$, where the incident plane wave is of the form

$$u_{\text{inc}}(\mathbf{x}, t) = \cos(\vec{\omega} \cdot \mathbf{x}) \cos(\omega t) + \sin(\vec{\omega} \cdot \mathbf{x}) \sin(\omega t).$$

We have set the propagation direction $\vec{\omega} = \omega(-\frac{\sqrt{2}}{2}, \frac{\sqrt{2}}{2})$, and the stopping criterion is achieved when relative euclidean norm of the gradient of the functional J is less than 10^{-5}. Error due to geometry modeling is reduced to an insignificant level by using geometries with polygonal boundaries.

Large time step allows to compute the solution utilizing only small amount of CPU time, but it may involve an error which deteriorates the accuracy of the method. Because of accuracy and stability demands the time interval $[0, T]$ is divided into 300 time steps ($\Delta t = 1/600$) in the case of central finite difference (CD) time discretization and into

150 time steps ($\Delta t = 1/300$) in the case of Runge-Kutta (RK) time discretization. The results are obtained by using a PC based on an AMD Athlon XP 1800+ CPU at 1.5 GHz.

As a smoother of the AMG we have used successive over relaxation (SOR), with over-relaxation parameter 1.2. One iteration of SOR is used as pre- and post-smoothing. Additionally, in the beginning of every multigrid iteration, four iterations of SOR is used to smooth the solution initially. In this case, so called W-cycle[12] is utilized as a multigrid iteration.

6.1 Accuracy

To study the effect of spatial and temporal discretizations we eliminate the error of absorbing boundary condition by modifying the scattering problem such that we know the solution u to be the plane wave u_{inc}. To achieve this, we introduce a function $g \in H^1(\Omega)$ such that $g|_{\Gamma_0} = u_{\text{inc}}$, $g|_{\Gamma_{\text{ext}}} = 0$ and $\frac{\partial g}{\partial \mathbf{n}}|_{\Gamma_{\text{ext}}} = 0$, and define $\hat{u} = u - g$. Then, function $\hat{u}$ satisfies the wave equation

$$\frac{\partial^2 \hat{u}}{\partial t^2} - \nabla^2 \hat{u} = -\frac{\partial^2 g}{\partial t^2} + \nabla^2 g$$

and the boundary conditions (5) and (6). We use the controllability algorithm to compute the function $\hat{u}$ and, in the end, get the actual solution u by the summation $\hat{u} + g$.

We use a mesh with stepsize $h = 1/4$ to solve this modified test problem with wavenum-

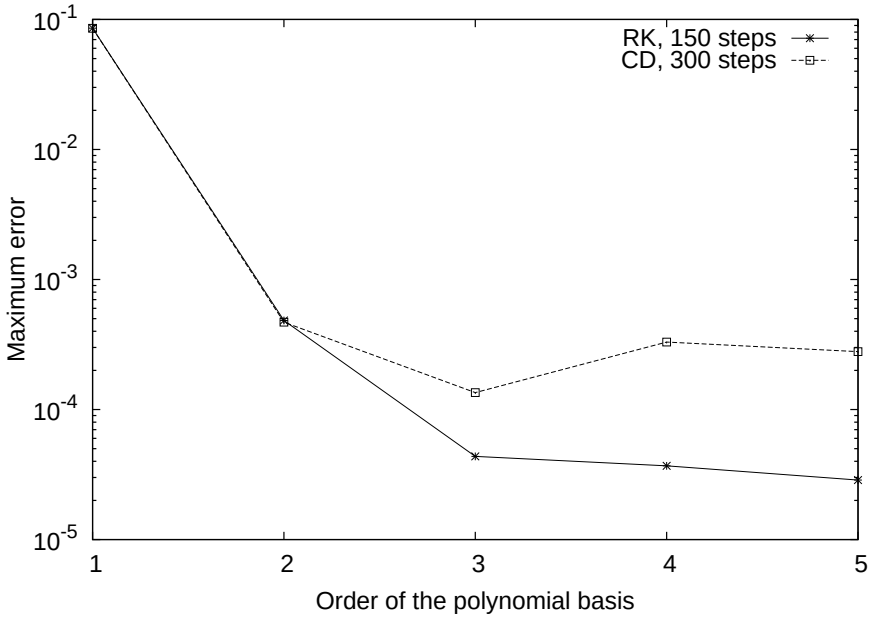

Figure 1: L_∞-norm of the difference between analytic solution and numerical solution with respect to the spectral order.

ber $\omega = \pi$ and time interval $[0, 2]$. The boundary Γ_{ext} coincides with a rectangle with the lower left corner at the point $(0.0, 0.0)$ and the upper right corner at the point $(4.0, 4.0)$. In the center of this rectangle, we have a bounded square scatterer with side length 2.

Figure 1 shows the error when the order of the spectral basis is increased. As the order increases, the error decreases until the error of the time discretization or the stopping criterion is achieved. According to Figure 1, error of spatial discretization dominates with low order elements. Thus, the difference between maximum errors is negligible for spectral orders $r = 1$ (corresponding to bilinear finite elements) and $r = 2$. When higher order elements are used, results computed with RK version of the algorithm are more accurate than the ones computed with the CD version.

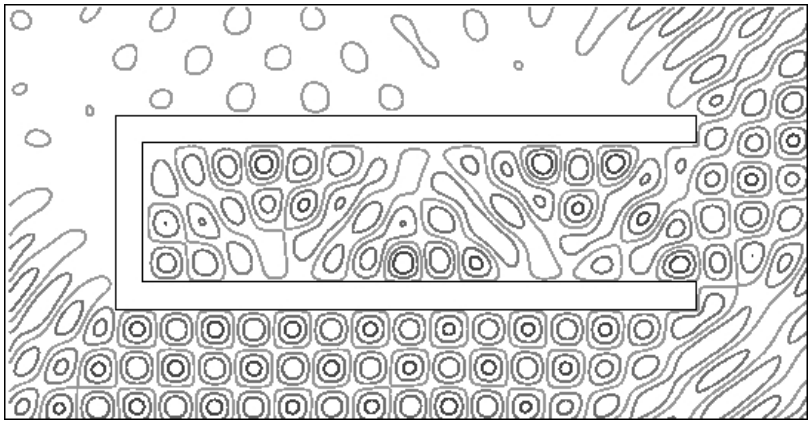

Figure 2: Contourplot of scattering by a non-convex semi-open cavity.

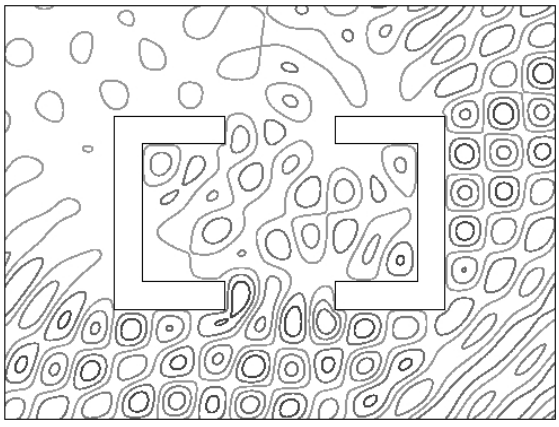

Figure 3: Contourplot of scattering by two non-convex semi-open cavities.

6.2 Scattering by non-convex cavities

We consider acoustic scattering by a non-convex semi-open cavity and a system of two semi-open cavities with angular frequency $\omega = 4\pi$, total time $T = 1/2$, and mesh stepsize $h = 1/32$. In the first scattering test, the lower left corner of the surrounding domain is at the point $(0.0, 0.0)$ and the upper right corner is at the point $(7.25, 3.75)$. Internal width and height of the cavity are 5 and $\frac{5}{4}$, respectively, and thickness of the wall is $\frac{1}{4}$ (see Figure 2). As the second test case, we solve the same problem in a domain, where the artificial boundary Γ_{ext} coincides with the border of a quadrangle $[0, 5] \times [0, 4]$, and we have two non-convex semi-open cavities as scatterers. Internal width and height of each cavity are $\frac{3}{4}$ and $\frac{5}{4}$, respectively. Thickness of the wall is $\frac{1}{4}$, and distance between cavities is 1 (see Figure 3).

Both test examples are solved by increasing the order of the spectral element basis. Figures 2 and 3 represent the total field u obtained by the RK time discretization and cubic spectral element basis ($r = 3$). The number of CG iterations needed to solve the control problem with CD and RK time discretizations are compared in Table 1, which also shows the number of degrees of freedom (DOF) in the spectral element mesh. The choice of the geometry of the scatterer affects the number of iterations. In the case of one non-convex semi-open cavity more reflections are produced inside the cavity than in the case of two non-convex semi-open cavities. Therefore, the number of iterations in the first test example is more than twice as large as in the second test example. The number of iterations is almost the same with both time discretizations. Since the preconditioner accelerates the convergence rate of the CG method, the number of preconditioned CG iterations is independent of polynomial degree r.

CPU time in seconds is depicted in Figure 4, where DOF increases as the order of the spectral element basis increases from 1 to 3. Solving the system with inversion of the mass matrix $\mathcal{M}^{-1}$ is required only once at each timetep in CD time discretization, whereas in the case of RK time discretization each time step involves four multiplications by $\mathcal{M}^{-1}$. This allows to use larger stepsizes in RK with good accuracy, but it also increases the

	r	1	2	3
test 1	DOF	25568	100800	225696
number of	RK	321	303	299
iterations	CD	351	330	326
test 2	DOF	18039	71151	159335
number of	RK	153	146	145
iterations	CD	156	147	144

Table 1: Number of iterations in the case of a non-convex semi-open cavity (test 1) and two non-convex semi-open cavities (test 2) with mesh stepsize $h = 1/32$ and angular frequency $\omega = 4\pi$.

computational effort when compared to CD. Although the RK version of algorithm needs more CPU time than the CD version, computational efforts of the methods with CD and RK time discretization are of the same order of magnitude.

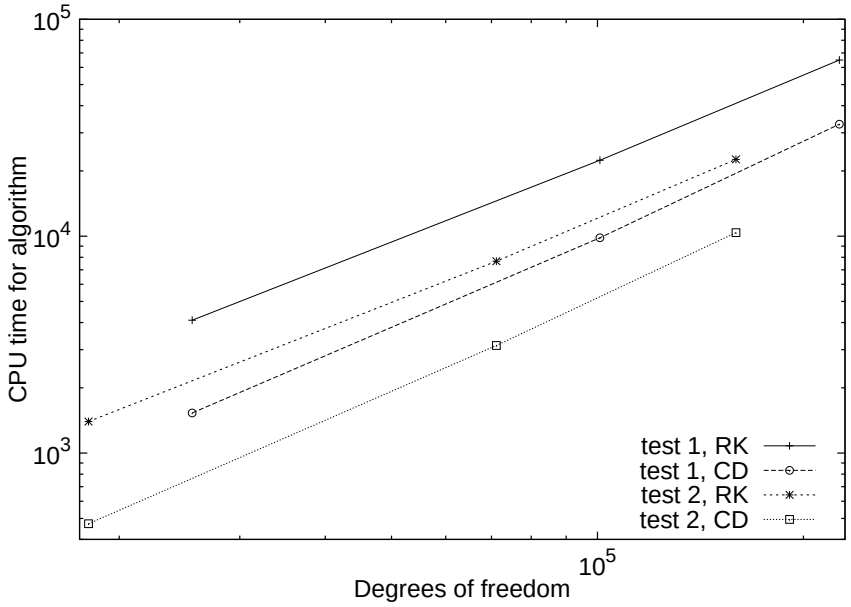

Figure 4: CPU time in seconds with respect to the number of degrees of freedom.

7 CONCLUSIONS

The spectral element formulation used in this article results in a global mass matrix that is diagonal by construction. No inversion of a mass matrix is needed either in the method with CD or in the method with RK time discretization. This leads to efficient implementation, which is an advantage compared to classical finite element method.

Simulation results show that the number of CG iterations is independent of the number of optimization variables, i.e. two times DOF. The method with RK time discretization needs more computational time, but leads to more accurate result than the method with CD time discretization. CPU times of both methods are of the same order and seem to depend linearly on DOF.

Acknowledgements

The authors thank Dr. Jari Toivanen and Dr. Janne Martikainen for useful discussions.

References

[1] G. Cohen. *Higher-Order Numerical Methods for Transient Wave Equations*. Springer Verlag, 2001.

[2] E. Heikkola, S. Mönkölä, A Pennanen, and T. Rossi. Solving the acoustic scattering problem with controllability and spectral element methods. Reports of the Department of Mathematical Information Technology, Series B. Scientific Computing, B 3/2006, Department of Mathematical Information Technology, University of Jyväskylä, 2006.

[3] M. O. Bristeau, R. Glowinski, and J. Périaux. Controllability methods for the computation of time-periodic solutions; application to scattering. *Journal of Computational Physics*, 147(2):265–292, 1998.

[4] E. Heikkola, S. Mönkölä, A. Pennanen, and T. Rossi. Controllability method for acoustic scattering with spectral elements. *Journal of Computational and Applied Mathematics*. To appear.

[5] J. L. Lions. Exact controllability, stabilization and perturbations for distributed systems. *SIAM Review*, 30(1):1–68, March 1988.

[6] Y. Maday and A. T. Patera. Spectral element methods for the incompressible Navier-Stokes equations. In A. K. Noor and J. T. Oden, editors, *State-of-the-art surveys on computational mechanics*, pages 71–143, New York, 1989. American Society of Mechanical Engineering.

[7] G. Mur. The finite-element modeling of three-dimensional electromagnetic fields using edge and nodal elements. *IEEE Transactions on Antennas and Propagation*, 41(7):948–953, 1993.

[8] F. Kickinger. Algebraic multi-grid for discrete elliptic second-order problems. In *Multigrid methods V (Stuttgart, 1996)*, pages 157–172. Springer, Berlin, 1998.

[9] J. Martikainen and A. Pennanen. Application of an algebraic multigrid method to incompressible flow problems. Reports of the Department of Mathematical Information Technology, Series B. Scientific Computing, B 2/2006, Department of Mathematical Information Technology, University of Jyväskylä, 2006. Submitted to Journal of Computational Physics.

[10] J.J. Heys, T.A. Manteuffel, S.F. McCormick, and L.N. Olson. Algebraic multigrid for higher-order finite elements. *Journal of Computational Physics*, 204(2):520–532, 2005.

[11] J. W. Ruge and K. Stüben. Algebraic Multigrid (AMG). In Stephen F. McCormick, editor, *Multigrid Methods*, Frontiers in Applied Mathematics, pages 73–130. SIAM, Philadelphia, Pennsylvania, 1987.

[12] W. Hackbusch. *Multigrid Methods and Applications*. Springer-Verlag, Berlin, Germany, 1985.